

ULTRASTRUCTURAL ALTERATIONS ON THE PLATELET SURFACE INDUCED BY COMPLEMENT MEMBRANE ATTACK COMPLEX, DEMONSTRATED WITH SERIAL SECTIONS AFTER CRYOFIXATION AND CRYOSUBSTITUTION

E. Morgenstern^{1*}, P.A. Holme², K. Høgåsen³, R. Dierichs⁴ and N.O. Solum²

¹Department of Medical Biology, Faculty of Medicine, University of Saarland, Homburg, Germany, ²Research Institute for Internal Medicine, University of Oslo, ³Institute of Immunology and Rheumatology, University of Oslo, Rikshospitalet, Oslo, Norway, ⁴Institute of Anatomy, University of Münster, Münster, Germany

(Received for publication June 1, 1996 and in revised form December 20, 1996)

Abstract

The membrane attack complex C5b-9 (MAC) induces cell permeabilization accompanied by shedding of "microparticles" from the plasmalemma. We used cryofixation and examination of serial sections to demonstrate the ultrastructural details of the complement mediated alterations. The complement system was activated by incubation of citrated platelet rich plasma with the antibody IgM FN 52 to CD9. The experiment was monitored with an aggregometer, and arrested by rapid freezing during (1) shape change and (2) increasing light transmission. Phase 1 was characterized by filopodia formation, degranulation, and irregularities of the plasmalemma. Sequestration of cytoplasmic fragments was detected infrequently. In phase 2, the cytosol became electron lucent. Sequestration of cytoplasmic fragments from the platelet body appeared frequently. Membrane-attached electron dense deposits and distinct particles with a dimension similar to that of the MAC were recognized on the membranes. In the neck region of sequestered fragments, stretched membrane-like lines inserted angularly into the membrane were found. From their structural and dimensional characteristics, it was concluded that they represent an end to (membrane) site position of the MAC during sequestration. The findings suggested that membrane alterations were induced in early phases by permeabilizing precursors, and later by the incorporation of the complex into the membrane. This led to a decrease in cytosol density, which agreed with increasing light transmission in the aggregometer.

Key Words: Blood platelets, complement membrane attack complex, cryofixation/substitution.

*Address for correspondence:

E. Morgenstern
Medizinische Biologie, Universität des Saarlandes
D-66421 Homburg/Saar, Germany

Telephone number: +49-06841-166252

FAX number: +49-06841-166227

E-mail: em@rz.uni-sb.de

Introduction

The complement membrane attack complex C5b-9 (MAC), which is known to be essential in host defence mechanisms, efficiently induces membrane permeabilization. After complement activation, the MAC is formed by the molecular fusion of the five terminal complement proteins, C5, C6, C7, C8 and C9 (reviewed in Esser, 1994). The resulting complex converts into a circular structure that looks identical to a ring of oligomerized C9, poly (C9), when imaged in the electron microscope (Podack and Tschopp, 1984; Mueller-Eberhard, 1985; Tschopp *et al.*, 1986). The MAC is able to insert into the cell membrane with its hydrophobic faces (Mueller-Eberhard, 1985; Peitsch *et al.*, 1990; Esser, 1994). During membrane interaction of the MAC, the shedding of so-called microparticles from the plasmalemma of platelets was described (Sims *et al.*, 1988, 1989a,b; Wiedmer *et al.*, 1990; Wiedmer and Sims, 1991; Holme *et al.*, 1993; Solum *et al.*, 1994) and other cells (Podack and Tschopp, 1984; Mueller-Eberhard, 1985; Morgan *et al.*, 1987; Boom *et al.*, 1989; Kerjaschki *et al.*, 1989; Malinski and Nelsestuen, 1989; Hamilton *et al.*, 1990; Young and Young, 1990; Hamilton and Sims, 1991; Halperin *et al.*, 1993). Up until now, a direct electron microscopic demonstration of the permeabilization process is lacking. In this study on platelets, complement activation was induced by addition of a monoclonal IgM class antibody (FN 52) against CD9. This was done in an aggregometer, which offers the advantage that the permeabilization can be observed as highly reproducible curves representing variations in light transmission. Serial sections of platelets were examined in order to obtain direct information about the ultrastructural details of MAC insertion into the membrane and of the shedding process during the various phases of membrane permeabilization. Chemical fixation with aldehydes provokes membrane vesiculation itself (Morgenstern, 1991). Therefore, we wanted to capture the action of the permeabilizing MAC on platelets with rapid freezing with a time arrest of < 1 milliseconds.

Materials and Methods

Platelet-rich plasma (PRP) was obtained by centrifugation of citrated blood (0.013 M trisodium citrate) at

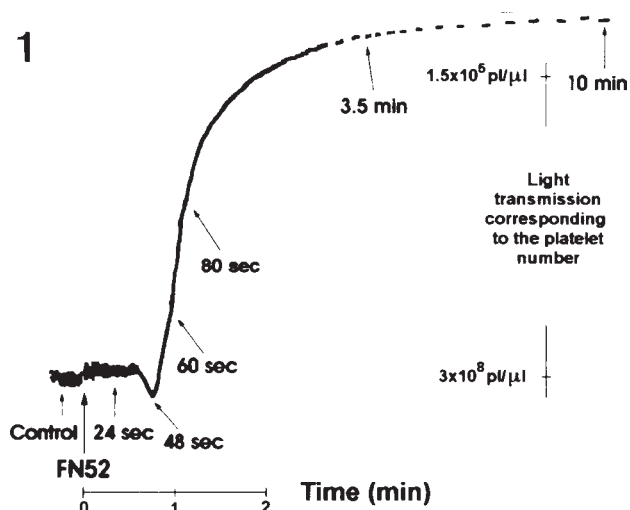


Figure 1. Aggregometer curve (for details, see text in the section **Aggregometer curve**).

320 g for 15 minutes. The complement system was activated by addition of a monoclonal IgM class antibody (FN 52; Solum *et al.*, 1994) directed towards the membrane antigen CD9 to the platelet suspension at 37°C. The platelet response was monitored as aggregometer curves which were highly reproducible, as long as the same PRP and concentration of the antibody were used.

The aggregometer (Chrono-Log Dual Channel Model 440, Chrono-Log Corporation, Havertown, PA) was calibrated in such a way that the difference in signal between PRP (3×10^8 platelets/ μl) and platelet-free plasma corresponded to 80 recorder chart divisions.

Complement activation was induced by addition of 25 μl of a 1/50 dilution of FN 52 ascites in Tris-buffered saline, pH 7.4, to 475 μl PRP in the aggregometer during magnetic stirring at 37°C (for further details, see Solum *et al.*, 1994). For electron microscopy, samples of 20 μl were withdrawn directly from the aggregometer cuvette in three consecutive runs with the time intervals from addition of FN 52 indicated on the aggregometer curve in Figure 1.

To obtain a more concentrated platelet suspension, one experiment was performed with platelets from a three day-old acid-citrate-dextrose platelet concentrate (Red Cross Blood Center, Rikshospitalet, Oslo) with the platelets sedimented and resuspended in citrated plasma to a platelet density of 1×10^9 platelets/ μl . Otherwise the experimental procedure was as described above for the platelet-rich plasma.

The platelet reaction was arrested by rapid freezing without prior fixation with the metal-mirror attachment MM 80 to the KF 80 cryofixation unit (Reichert-Jung/Vienna, Austria)

as described in Morgenstern and Edelmann, 1989). The samples were then freeze-substituted in acetone containing 4% (w/v) osmium tetroxide and 0.25% uranyl acetate as well as, to enhance the staining of cytoskeletal elements (Ornberg and Reese, 1981), 0.1% hafnium chloride (Ventron Alpha Produkte, Karlsruhe, FRG) for 48 hours at 193 K with the AFS auto cryosubstitution unit (Reichert-Jung). The specimens were embedded in Araldite after rewarming. Ultrathin section series were prepared with an Ultracut E (Reichert-Jung) ultramicrotome. Ultrathin serial sections were stained with uranyl acetate and lead citrate.

Computer-assisted 3-dimensional reconstruction from serial sections was carried out using a Kurta IS/ADB input system (Phoenix, AZ) and an Apple Macintosh Quadra 840 personal computer. The applied software was described in detail in Bogusch and Dierichs (1995).

Results

Aggregometer curve

As demonstrated in Figure 1, addition of the antibody to PRP results in an aggregometer curve that can be divided into different phases. In the following, we use the term light transmission to describe intensity of the light emerging from the platelet suspensions. On the ordinate, this is stated as light transmission corresponding to the number of platelets obtained when the original PRP is diluted with the homologous platelet free plasma. Starting from the left of the curve, a lag phase shows the regular oscillations observed with disc-shaped platelets. Then, the oscillations disappear concomitant with a decrease in light transmission.

The peak indicates a change in shape from discs to spheres. This is followed by an increase in the light transmission giving an ascending curve with practically no oscillations. This effect was attributed (1) to the induced degranulation and (2) to the membrane permeabilization induced by activation of the complement system and associated with a leakage of components of the platelet cytoplasm. With the concentration of the complement activating antibody used, the formation of aggregates could not be observed (Solum *et al.*, 1994).

Ultrastructural observations

The following descriptions, as well as the presented micrographs and reconstructions are related to platelets from citrated PRP. The findings on the platelets obtained from a platelet concentrate (control as well as 60 seconds, 2.5 and 10 minutes after FN 52-addition) resemble the described observations, but are not shown.

The untreated control platelets show the section profiles of discocytes, the marginal bundle of microtubules, the surface connected system and the dense tubular system, as well as regular cell organelles (α -granules, dense granules and mitochondria). In Figures 2a-2c, the regular aspect of the

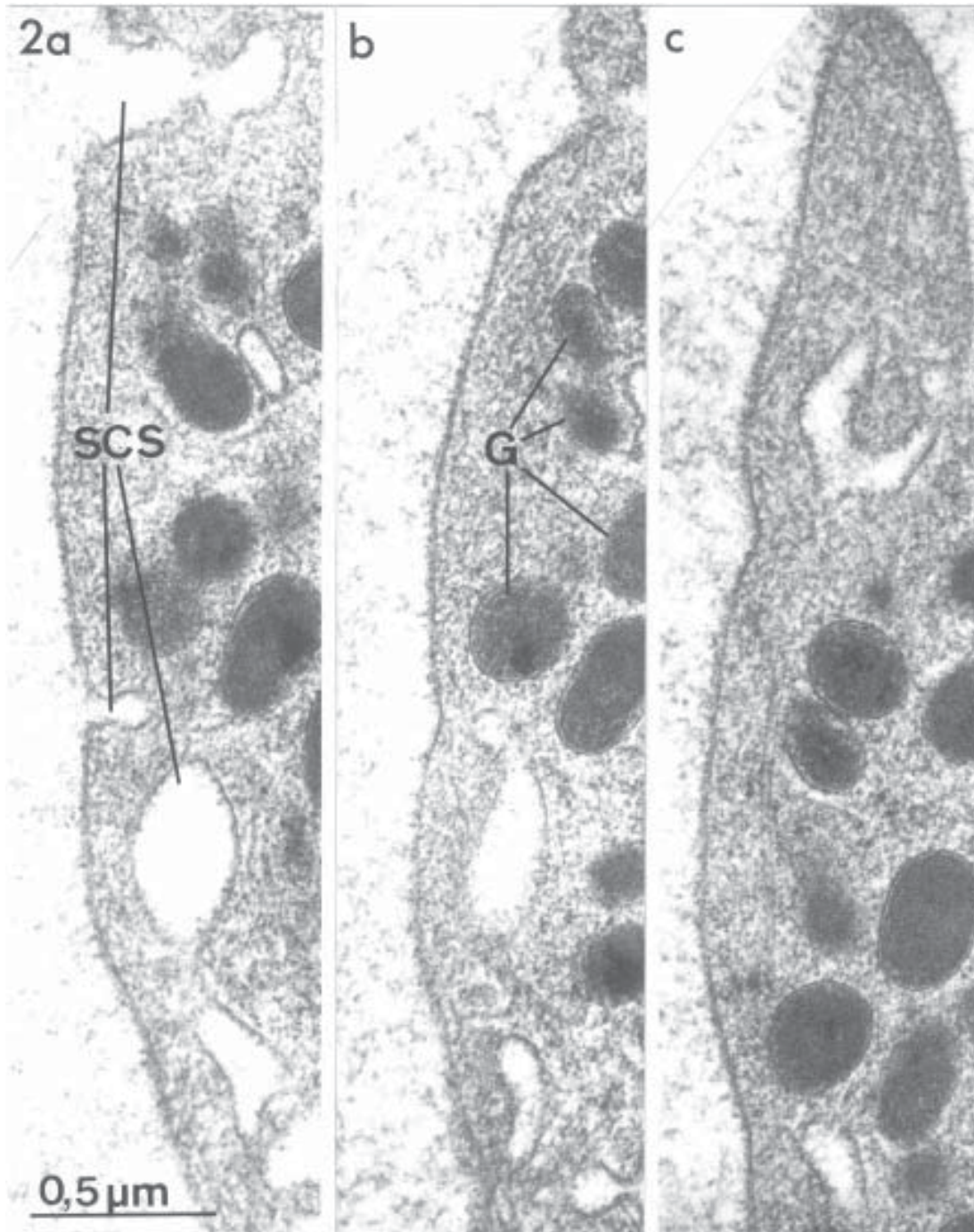


Figure 2 (a-c). Three serial sections from a control platelet show the smooth and continuous regular structure of the plasmalemma. A system of surface connected membranes with its openings to the plasmalemma is indicated in **Figure 2a (SCS)**. The secretory organelles (alpha-granules) are indicated in **Figure 2b (G)**.

platelet plasmalemma is demonstrated to allow a comparison with the FN 52-treated cells.

The observed ultrastructural alterations after activation

of the complement system concern (a) platelet activation (shape change with formation of filopodia and degranulation), (b) plasmalemmal irregularities, (c) the sequestration of

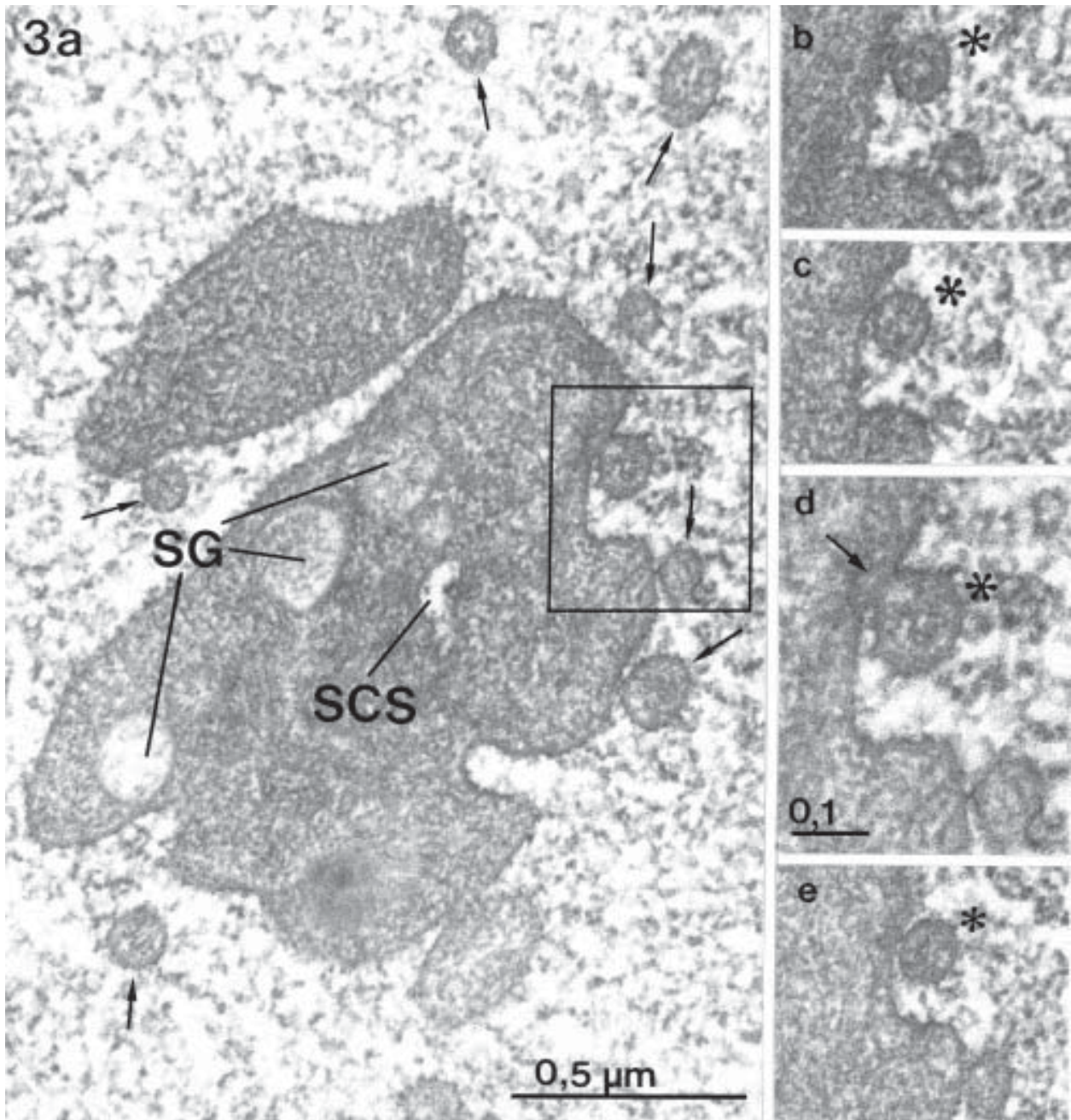


Figure 3 (a-e). Serial sections of a platelet in the shape change phase (48 seconds after addition of FN 52) show a platelet that is rounded off but is surrounded by a remarkable number of circular cytoplasmic profiles (arrows in **Fig. 3a**). Only small remnants of the surface connected system (SCS) are present and swollen alpha-granules during exocytosis (SG) are seen in **Figure 3a**. The serial sections in **Figures 3b-3e** (see inset in **Fig. 3a**) demonstrate that one of the surrounding profiles (asterisks) is connected with the platelet cytoplasm by a thin neck (arrow in **Fig. 3d**) only visible in a single section. Compare the reconstruction in Figure 4 for interpretation.

cytoplasmic fragments and (d) a decreasing electron density of the cytosol.

Shape change with formation of filopodia and

degranulation: After 48 seconds (Figs. 3a-3e), the maximum shape change is reached. The channels of the surface connected system are drastically reduced, and the cells appear

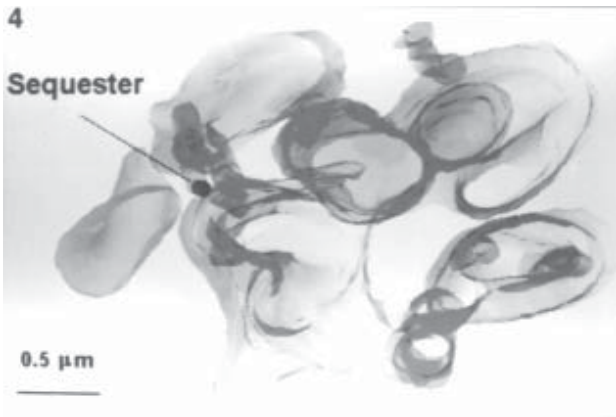
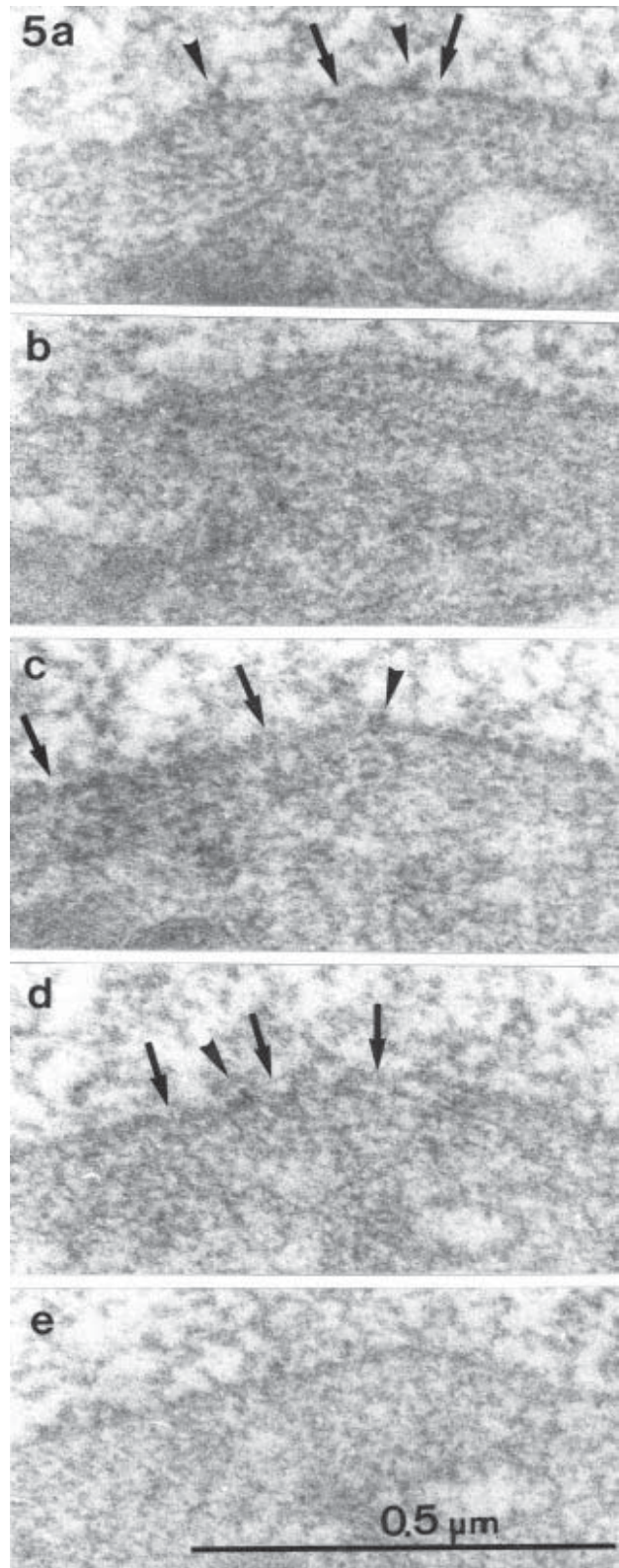


Figure 4. The three-dimensional (3D) reconstruction from 12 sections of a platelet in the shape change phase (48 seconds after addition of FN 52, cf. Fig. 3a). The reconstruction demonstrates long filopodia, and that most of the circular profiles, seen in the sections, are due to filopodia. Only the indicated small sequester was clearly found to be separated from the platelet body.

Figure 5 (a-e; at right). The contour of the plasmalemma of a platelet prior to shape change (24 seconds after addition of FN 52) is shown in five consecutive sections. In **Figures 5a, 5c and 5d**, arrows indicate depressions or discrete interruptions of the lipid bilayer. The arrowheads in **Figures 5a, 5c and 5d** indicate irregular electron dense structures in the membrane contour.



partly degranulated. The hyaloplasm shows unaltered electron density (cf. Fig. 2 and see **Decrease of density of the cytoplasm** below). The platelets have formed long, thin pseudopodia (filopodia). Numerous circular profiles are seen around the platelets. The 3D-reconstruction (Fig. 4) demonstrates long filopodia and that most of the circular profiles, seen in the sections (Fig. 3a), are due to filopodia. Sequestration of cytoplasmic fragments from the cell surface is very seldom recognizable (Fig. 3d). The number of cells in such a state is drastically decreased after longer incubation periods. Then, the platelets round off and increasingly show an electron lucent cytosol, sequestration events and a decreasing number of pseudopodia {compare Fig. 3a with Fig. 7a (shown later)}.

Plasmalemmal irregularities: After 24 sec, the platelets in our experiments persisted in the discoid state. However, compared to control platelets, the contour of the plasmalemma shows distinct interruptions of the lipid bilayer and irregular dense structures in serial sections (Figs. 5a-5e). Such plasmalemmal irregularities are recognizable on platelets in the phase of shape change.

Later, in cells with increasing electron lucency of the

cytosol, pronounced irregularities are recognizable (Figs. 6a-6e and 7a-7e).

Electron dense material on the cytoplasmic face of the

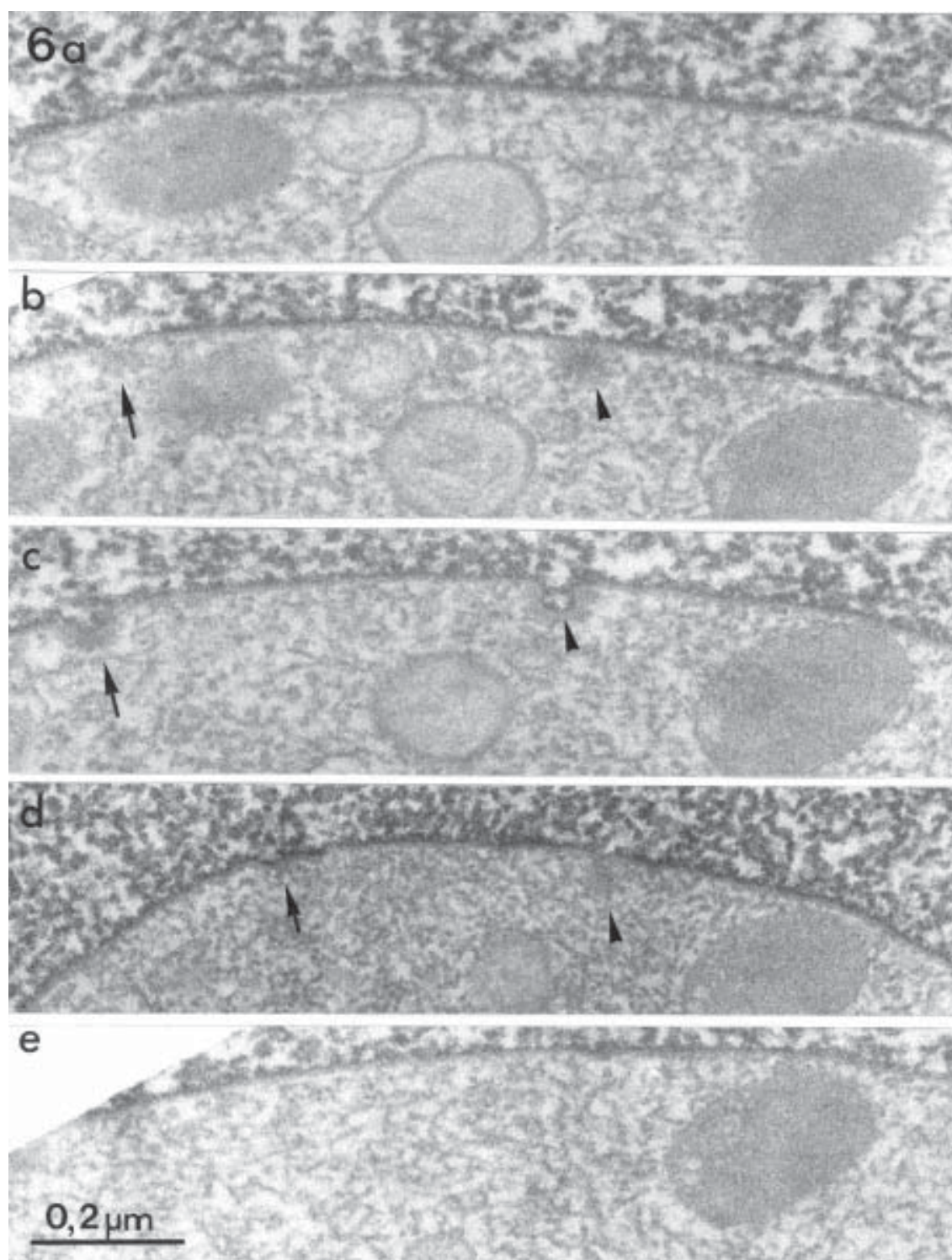


Figure 6 (a-e). Serial sections of a platelet with an electron lucent cytoplasm (60 seconds after addition of FN 52) shows two membrane irregularities (arrows and arrowheads in sections **Figs. 6b-6d**). These remind one of a coated pit (**Fig. 6c**) but does not show its regular dimension (approximately 30 nm instead of 70-100 nm in diameter). The dense deposits reveal a serrated rim (arrowheads in **Figs. 6b-6d**) and at the site of their insertion the membrane contour appears to be interrupted (arrowhead in **Fig. 6d**).

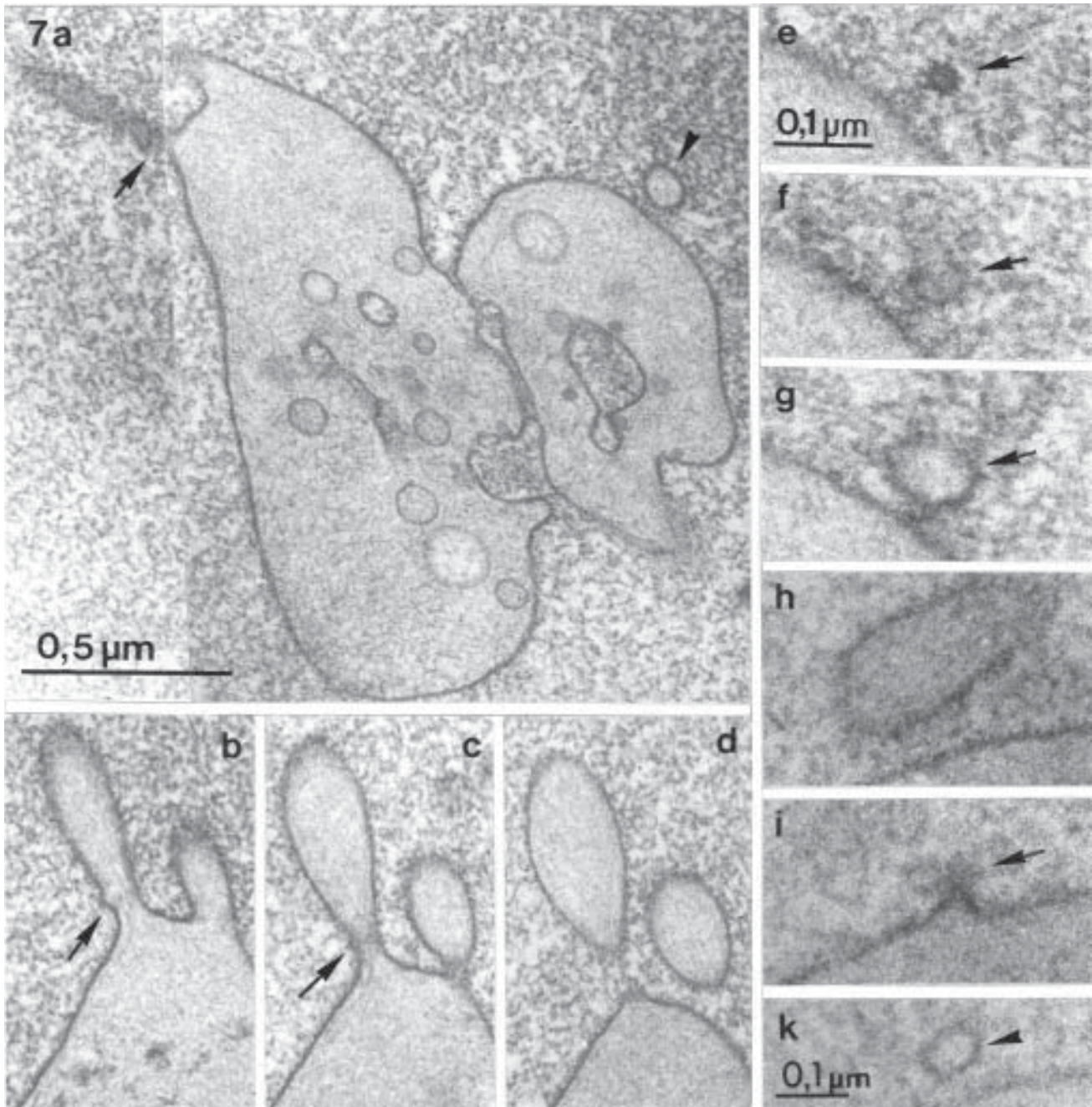


Figure 7 (a-k). Serial sections of a platelet in a late phase (80 seconds after addition of FN 52) shows a degranulated cell with electron lucent cytoplasm. In **Figure 7a**, the sequestration of two elongated fragments is seen, demonstrated in three consecutive sections (**Figs. 7b-7d**). The arrows in **Figures 7a-7c** indicate membrane irregularities with dense deposits on the outside of the neck membrane. Three further sections (**Figs. 7e-7g**) from the separated fragment (indicated in **Fig. 7a** with an arrowhead) are shown (arrows). The section in **Figure 7e** shows a serrated dense particle (30 nm in diameter) that might be associated with the membrane of the fragment as demonstrated in the sections in **Figures 7f and 7g**. In the consecutive sections (**Figs. 7h-7k**), the arrow in **Fig. 7i** indicates a serrated density at the site of the sequestration of a small fragment (arrowhead in **Fig. 7k**).

Note: Scale bars are indicated in **Figures 7a** (for **Figs. 7a-7d**), **7e** (for **Figs. 7e-7g**), and **7k** (for **Figs. 7h-7k**).

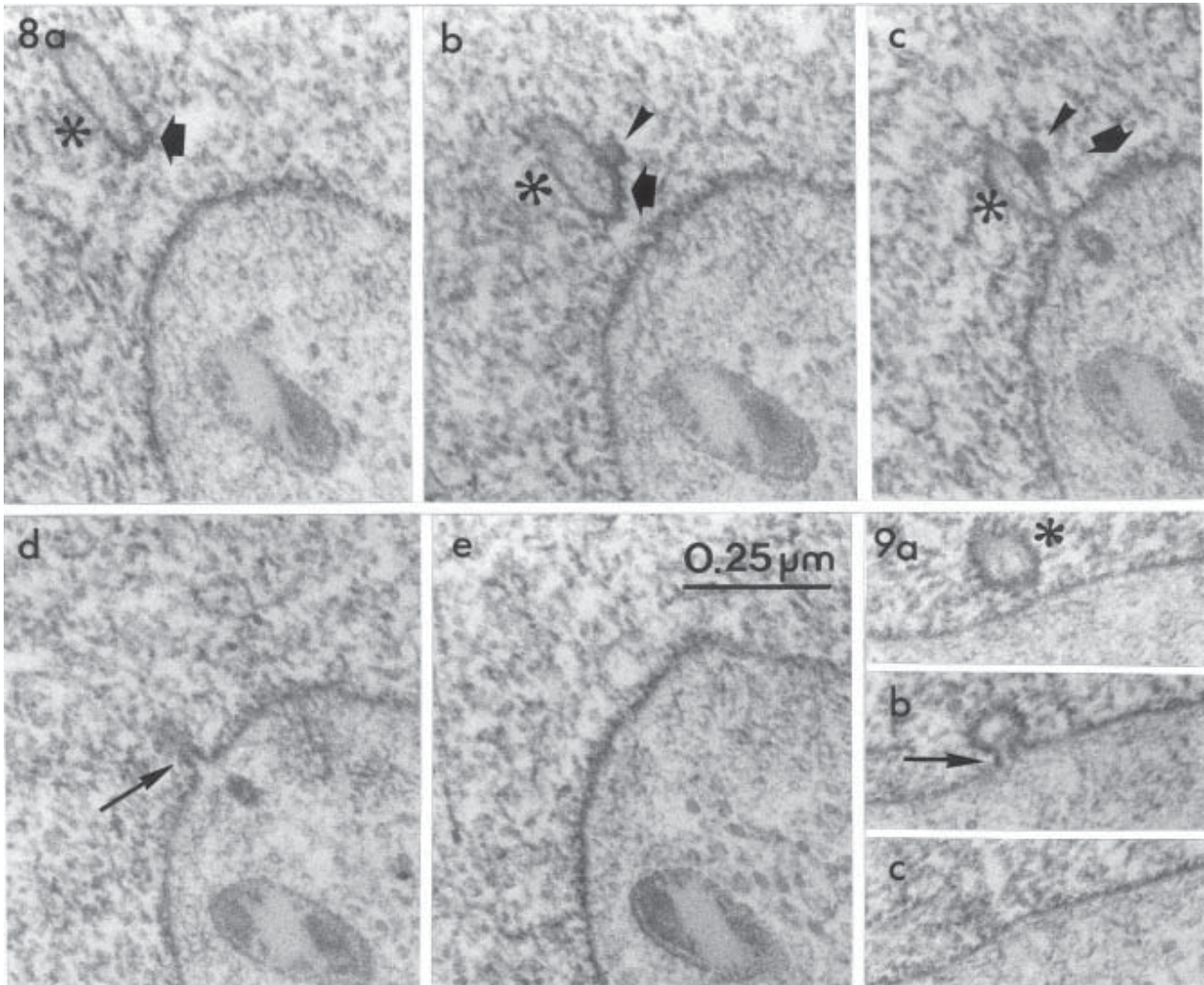


Figure 8 (a-e). Serial sections of a platelet with an electron lucent cytoplasm (60 seconds after addition of FN 52) show the sequestration of a fragment (asterisks in **Figs. 8a-8c**). An electron dense ring-like serrated structure (about 50 nm in diameter) is associated with the membrane of the fragment and indicated by arrowheads in **8b** and **c**. The elongated neck of the fragment that is only seen in **Figure 8d** is indicated with an arrow. There, the stretched appearing lines of the neck insert in an angular form into the membranes. Portions of the fragment membrane are covered with serrated dense deposits. In **Figure 8c**, the plasmalemma shows the deposition of electron dense material (thick arrow) and the plasmalemmal contour is not regular.

Figure 9 (a-c at bottom right). Three serial sections from a platelet prepared as in Figure 8 show a further example of sequestration. The fragment is indicated in **Figure 9a** (asterisk). The elongated neck of the fragment is only seen in **Figure 9b** (arrow). The stretched appearing lines of the neck insert in an angular form into the membranes.

plasmalemma is a frequent and characteristic finding at the site of membrane irregularities. Some irregularities remind one of a coated pit (Fig. 6c) because the cytoplasmic dense deposits appear to be serrated. However, these structures (approximately 30 nm in diameter) do not show the regular dimension of coated pits (70-100 nm in diameter). In some

cases, the membrane contour may be interrupted (Fig. 6d).

Dense, serrated deposits that cover the extracellular face of the plasmalemma (shown in Fig. 8c) or the membrane of fragments are often observed (Figs. 7g, and 8a and 8b). Serrated densities are also recognizable at the site of the sequestration of fragments (Fig. 7i). Serrated particles are

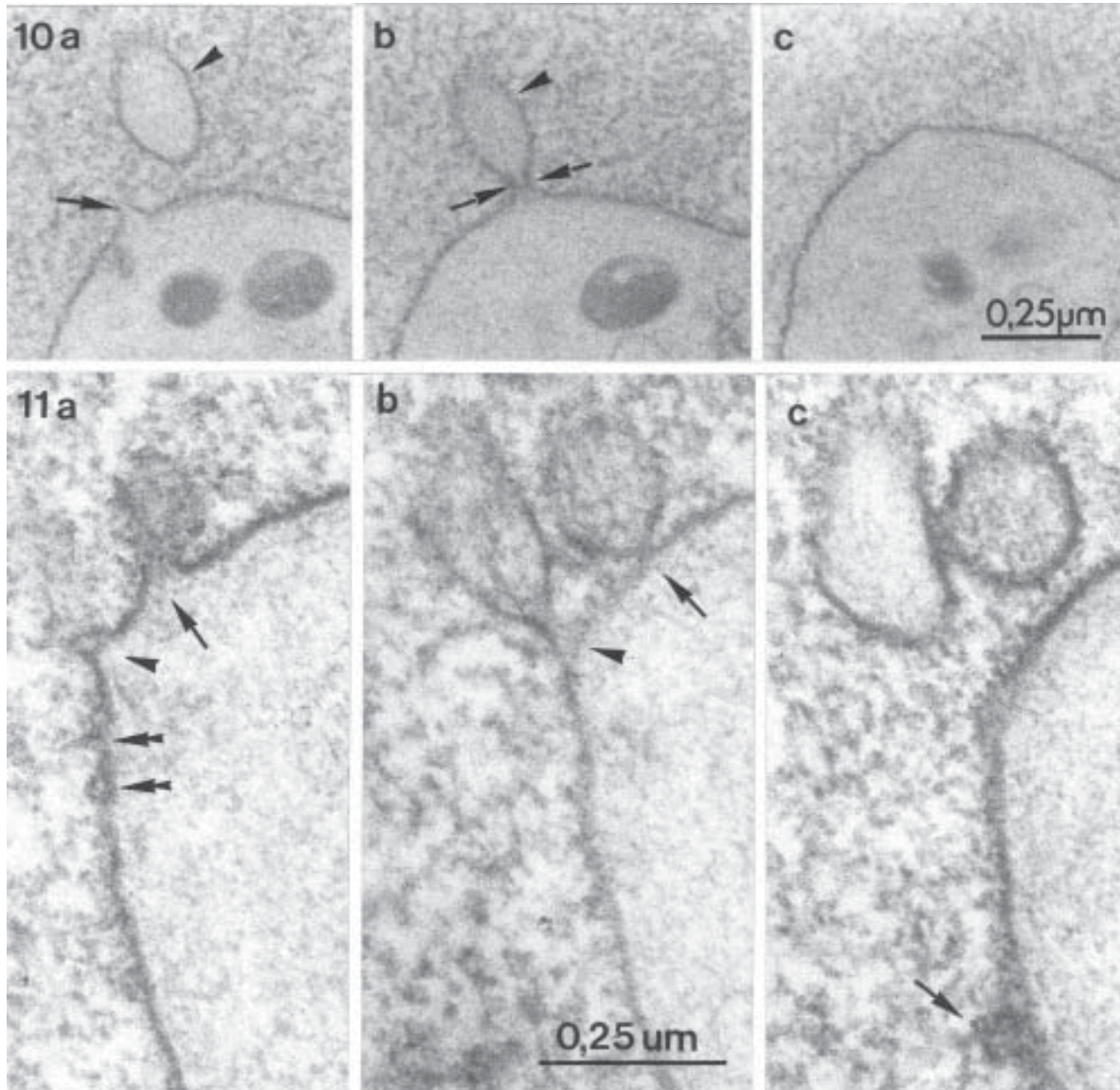


Figure 10 (a-c). Three consecutive sections of a platelet as shown in Figure 7 (80 seconds after addition of FN 52) demonstrate the formation of a fragment (arrowheads in **Figures 10a and 10b**). The membrane-like lines of the elongated neck of the fragment are pronounced by higher density compared with the membrane (arrows in **Fig. 10b**). The arrow in **Fig. 10a** indicates another site of the start of a sequestration as recognized in further sections (not shown).

Figure 11 (a-c). The section series of a platelet (80 seconds after addition of FN 52) shows a cell with electron lucent cytoplasm. The sequestration of two elongated fragments is demonstrated in three subsequent sections. The arrows and arrowheads in **Figures 11a and 11b** indicate the sites of formation of elongated necks on the fragments during sequestration. In section in **Figure 11a**, the two double arrows indicate annular structures within the membrane contour. The arrowhead in **Figure 11a** indicates that an annular membrane structure corresponds to the site of neck seen in **Figure 11b**. In section in **Figure 11c**, a serrated particle is associated with the plasmalemma (arrow).

found to be associated with the membrane of fragments as shown in Figures 8a-8c and 9a and 9b, as well as with the

plasmalemma (Fig. 11c, shown later). Moreover, already sequestered fragments show serrated dense particles

associated with their surrounding membrane (Fig. 7e). The dimension of these particles is in a range of 30-70 nm. The particle structure indicated in Figures 8b and 8c may be one elongated particle with a short axis of 40-50 nm. However, considering a section thickness of about 50 nm, its long axis may be longer than 70 nm. On the other hand, the serial technique does not permit a decision as to whether or not this structure represents two separate particles, or only one.

Another type of irregularity is the appearance of circular dense profiles with an internal width of 6-10 nm within the plasmalemma (Figs. 8c and 11a).

Sequestration of cytoplasmic fragments: Fragments in the process of separation (Fig. 3c), or already separated from the platelet surface (see 3D-reconstruction in Fig. 4), are rarely detected in early phases of platelet reaction to complement activation (48-60 seconds). Careful examination of serial sections (as shown in Figs. 3a-3e) and the reconstruction (Fig. 4) showed that the sequesters in this state appear as small spherical fragments with a content resembling the cytoplasmic matrix. Later, sequestration is found to be very frequent. The sequesters bud, often in pairs, from the plasmalemma (Figs. 7a-7d, 8a-8e, 9a-9c, 10a-10c, 11a-11c and the 3D-reconstruction in Fig. 12). The neck region of budding fragments may be covered with electron dense deposits (Figs. 7a-7c) as described above.

A characteristic aspect at a site of sequestration is the frequently observed thin elongated neck (Figs. 8d, 9b, 10b and 11b) with tightly configured, straight-running membrane-like lines (distance between the neck-forming lines about 12 nm). The contour of these lines is slightly intensified. The thickened parts of the neck are delineated in parallel (as in the examples in Figs. 8d and 9b). Furthermore, they insert into the plasmalemma as well as into the membranes of fragments in an extraordinary, angular form (Figs. 8d and 9b).

The content of the fragments shows the aspect of the cytoplasm. In no case are platelet organelles recognizable within the sequestered fragments.

Decrease of density of the cytoplasm: Samples from the ascending part of the aggregometer curve contain an increasing number of platelets with a hyaloplasm that is less electron dense than the blood plasma (Figs. 7a-7d, 10a-10c and 11a-11c). After 10 minutes, only platelet ghosts are seen.

Discussion

The cryofixation technique used demonstrates that the action of the membrane-permeabilizing complement attack complex results in sequestration (shedding) of cytoplasmic fragments which are commonly named microparticles or microvesicles. The formation of cytoplasmic fragments is consistent with reports that these particles express surface-bound procoagulant activity and contain cytoskeletal and contractile proteins (Sims *et al.*, 1989b; Wiedmer *et al.*, 1990;

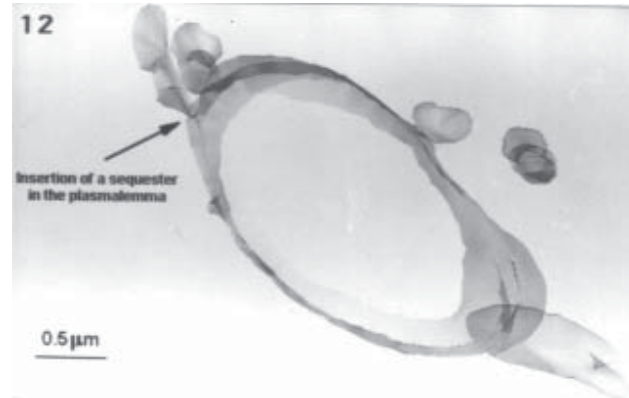


Figure 12. The 3D-reconstruction from of a platelet in a state with an electron lucent hyaloplasm demonstrates the sequestration (arrow) of elongated cytoplasmic fragments from the plasmalemma. The fragments seen in the right-hand of the platelet are found to be already sequestered in other points of view (not shown).

Holme *et al.*, 1993, 1994).

The sequestration events were most frequent after the cells had passed the shape change phase and showed an increased light transmission. In the present study, this corresponded to an incubation time with FN 52 of over 60 seconds. The continued membrane permeabilization leads to a decrease in electron density caused by leaching of cytosolic components or by water influx into the cytosol. This permeabilization effect agrees with the increasing light transmission in the aggregometer and the described liberation of adenosine triphosphate (ATP) during latelet reaction with FN 52 (Solum *et al.*, 1994).

This study focuses on the ultrastructurally recognizable signs of the MAC action. Therefore, the plasmalemmal irregularities are of particular interest as possible indications of the precursory steps of plasmalemmal injury by the MAC-forming molecules. Furthermore, the dense material on the cytoplasmic face of the membrane irregularities may indicate the action of such molecules.

Regarding the MAC formation, it was suggested that the complex of C5b-8 acts as a catalyst for C9 polymerization and that this complex is inserted into the poly(C9) ring (Tschopp, 1984; Podack, 1992). A poly(C9)-like configuration is also probable for the mature MAC. The molecular configuration of the MAC and its dimensions (28-30 nm in length) are described as comprising a 5-14 nm-wide tubule with a 18-21 nm-wide torus (annulus) at the top (Podack and Tschopp, 1984; Mueller-Eberhard, 1985). As to the mechanism of ring closure in the membrane, it was established that this is not required nor important for MAC-mediated membrane damage. Three to four C9 molecules per C5b-8 are completely sufficient to produce all known effects of the MAC, yet four

C9 molecules are insufficient to form a poly(C9) tubule (Esser, 1991, 1994). Other constituents of the C5b-9 complex, especially C8, may become incorporated into the cell membrane due to their amphiphilic character (Podack and Tschopp, 1984; Sodetz, 1988) and induce membrane permeabilization.

Complement proteins that are precursors of the MAC may act during early phases of FN 52-induced complex formation (24-48 seconds in this study). Discrete interruptions of the membrane contour indicate the permeabilization effect, which was postulated by others (see Esser, 1991). The presence of activated platelets undergoing shape change and degranulation and forming abundant filopodia during the first minute after addition of FN 52 is compatible with the findings of Wiedmer and Sims (1985) that incorporation of a few complexes in the plasmalemma induces repolarization and Ca²⁺-mediated platelet activation. However, the presence of rare sequestration events suggests that permeabilizing configurations of MAC or its precursors are already acting at this time. Interestingly, dense deposits on the sites of plasmalemmal irregularities are not recognizable during this early period. The absence of platelet aggregation indicates a serious disturbance of the membrane function. Obviously, the formation of receptor GPIIb/IIIa-ligand (fibrinogen) complexes is impossible. This suggestion is supported by observations with the monoclonal antibody PAC-1 that exclusively recognizes the activated form of the GPIIb/IIIa complex. This antibody bound to platelets incubated with FN 52 in the shape change phase, but was unable to bind at a later stage (Holme *et al.*, 1995).

After the shape change phase is over, and the platelets show increasing light transmission (> 60 seconds after addition of FN 52), more pronounced alterations on the plasmalemma are recognizable. First, membrane irregularities and sequestration of fragments are accompanied by associated electron dense deposits on the membrane. On the one hand, the deposits are observed on the cytoplasmic face of the plasmalemma where no sequestration of fragments takes place. There, the membrane-associated structures cover small membrane depressions and show a serrated rim resembling coated pits but with a dimension different from these. On the other hand, dense depositions are situated on the membrane surface. Both of these structural peculiarities are never recognizable in platelets stimulated by physiological agonists such as adenosine diphosphate (ADP) and collagen (Ruf and Morgenstern, unpublished observations) or, e.g., by an ionophore (Holme *et al.*, unpublished observations). Thus, the demonstrated deposits on the cytoplasmic face of the plasmalemma represent in all probability a consequence of the membrane attack by complement molecules.

A further conspicuous phenomenon is the appearance of serrated particles attached to the plasmalemma or to the membrane of fragments. Also at the site of sequestration, membrane-associated electron dense particles occur. They

are situated in the neck region of the sequestered fragments and are located on the extracellular face of the membranes. The occurrence of such particles has never been recognized on resting platelets, or platelets stimulated by ADP, collagen (Ruf and Morgenstern, unpublished observations) or an ionophore (Holme *et al.*, unpublished observations). The question arises as to whether these structures represent MAC complexes.

The dimension of particles (> 30 nm in diameter) calculated from micrographs of ultrathin sections in the present study is larger than the values for MAC structures obtained with other methods. Intramembrane particles (20-30 nm in size) were demonstrated in freeze-fracture replicas of aldehyde-fixed cell membranes after C5b-9 application (Humprey and Dourmashkin, 1969; Kerjaschki *et al.*, 1989). The dimension of such particles corresponds to the calculated size of the MAC, isolated from membranes and determined by negative staining electron microscopy (Biesecker *et al.*, 1979; Mueller-Eberhard, 1985; Podack and Tschopp, 1984). There, the dimension of the MAC is 10-21 nm in diameter and up to 30 nm in length. All these values were obtained using techniques that cannot exclude shrinking by aldehydes or alterations by isolation from membranes and by the negative staining procedure. Peitsch *et al.* (1990) have reconstructed the components of the MAC by molecular modelling. The estimated dimensions are compatible with the aforementioned dimensions. However, these methods may generate miscalculations.

A comparison of our values with those of others quoted above is critical. Of course, the sectioning technique may limit the chance to recognize the adequate dimension of structures. On the other hand, the cryofixation/substitution technique, the same as used here, was found to preserve the real dimensions of cell structures, e.g., the sarcomere dimension in resting and contracted muscle cells (for discussion, see Edelmann, 1989). Moreover, the information from the sections examined in this study reflects the situation *in situ*. This includes the interaction of MAC molecules with the membrane, probably with cytoskeletal elements and with components of the blood plasma. An enlargement of the MAC could be attributed to the conditions in the demonstrated specimens.

The observed surface-attached particles (MAC?) match the findings that MAC and precursor molecules bind to the surfaces of cells (Bhakdi and Trantum-Jensen, 1986). In nucleated cells, a removal of the MAC through endocytotic processes was reported (Carnoy *et al.*, 1985; Morgan *et al.*, 1987). In our investigation, no internalized particles were recognized in platelets. Sims and Wiedmer (1986) have suggested that platelets eliminate C5b-9 pores by exocytosis. The particles that were attached to, or inserted in the membrane of sequestered fragments in our study, may be the morphologic correlate of this phenomenon.

A third extraordinary finding concerns the thin necks

at the site of sequestration of cytoplasmic fragments. The parallel passage of the tightly approached membrane-like lines and their intensified contour in the neck region is striking. Also the angular insertion of the neck-lines into the plasmalemma as well as into the membranes of fragments are remarkable and do not correspond with the common behavior of a cell membrane. The necks of fragments in sequestration, that were observed in platelets stimulated by ADP, collagen (Ruf and Morgenstern, unpublished observations) or an ionophore (Holme *et al.*, unpublished observations) inconspicuously showed contours that inserted smoothly into the membranes. Such necks did not show the characteristics mentioned here after MAC-induction. The question arises as to whether these structures represent MAC complexes.

Supposing that the neck-lines are a product of the MAC, some details of these structures should be noted: (1) The distance between the stretched membrane-like lines (about 12 nm) corresponds to the lumen of the tubule in a MAC complex; its internal width was estimated between 5 to 14 nm (Podack and Tschopp, 1984; Mueller-Eberhard, 1985; Peitsch *et al.*, 1990). (2) The circular dense profiles with an internal width of 6-12 nm observed within the plasmalemmal contour agree with the dimension of a MAC tubule. (3) The enhanced density of the neck-lines and their angular insertion into the cell membrane suggests a structure different from a lipid-bilayer membrane.

In contrast to the findings during the first period of FN 52 influence (see above), the described structural details observed on the platelet surface indicate that the sequestration of cytoplasmic fragments in later phases is created by membrane incorporation of the mature MAC. The proteins of the MAC are amphiphilic and able to insert into the membranes. This is also the case for the C9 proteins that unfold upon interaction with the membrane-bound C5b-8 complex (Podack and Tschopp, 1984; Sodetz, 1988; Halperin *et al.*, 1988; Peitsch *et al.*, 1990). On the other hand, the possibility that the MAC traverses the membrane of cells completely (Tranum-Jensen and Bhakdi, 1983; Bhakdi and Tranum-Jensen, 1991) is still seriously discussed (cf. Esser, 1994). The observations in this study suggest that the necks of budding cell fragments are attributed to the MAC complex that enters the cell membrane in an end-to-side mode. This conformation might help to solve unanswered questions as to the action of MAC (see Esser, 1994). Such an arrangement of the MAC might establish a cytosolic connection between the cell and the sequestered fragments as well as provide the access of water to the charged faces of the MAC tubule and enable water influx into the cells or the fragments.

Acknowledgements

The authors wish to thank Dr. Ludwig Edelmann (Homburg) for advice in preparation and reading the

manuscript. We are grateful to Elin Rubach-Dahlberg, Turid M. Pedersen (Oslo) as well as to Anne Vecerde and Claudia Fischer (Homburg) for excellent technical assistance. The work was supported by The Norwegian Council on Cardiovascular Diseases, Anders Jahres Fund and Professor Paul A. Owrens Fund.

References

- Bhakdi S, Tranum-Jensen J (1986) C5b-9 assembly: Average binding of one C9 molecule to C5b-8 without poly-C9 formation generates a stable transmembrane pore. *J Immunol* **136**, 2999-3005.
- Bhakdi S, Tranum-Jensen J (1991) Complement lysis. A hole is a hole. *Immunol Today* **12**, 318-320.
- Biesecker G, Podack ER, Halverson CA, Mueller-Eberhard HJ (1979) C5b-9 dimer: Isolation from complement lysed cells and ultrastructural identification with complement-dependent membrane lesions. *J Exp Med* **149**, 448-458.
- Bogusch G, Dierichs R (1995) Outgrowing nerves in the foreleg of a mouse embryo as viewed by three-dimensional reconstruction from electron micrographs. *Cell Tissue Res* **280**, 197-209.
- Boom BW, Mommaas M, Daha MR, Vermeer BJ (1989) Complement-mediated endothelial cell damage in immune complex vasculitis of the skin: Ultrastructural localization of the membrane attack complex. *J Invest Dermatol* **93** (2 Suppl), 68S-72S.
- Carnoy DF, Koski CL, Shin ML (1985) Elimination of terminal complement intermediates from the plasma membrane of nucleated cells. The rate of disappearance differs for cells carrying C5b-7 or C5b8 or a mixture of C5b-8 with a limited number of C5b9. *J Immunol* **134**, 1804-1809.
- Edelmann L (1989) The contracting muscle: A challenge for freeze-substitution and low temperature embedding. *Scanning Microsc Suppl* **3**, 241-252.
- Esser AF (1991) Big MAC attack. Complement proteins cause leaky patches. *Immunol Today* **12**, 316-318.
- Esser AF (1994) The membrane attack complex of complement. Assembly, structure and cytotoxic activity. *Toxicology* **87**, 229-247.
- Halperin JA, Nicholson-Weller A, Brugnara C, Tosteson DC (1988) Complement induces a transient increase in membrane permeability in unlysed erythrocytes. *J Clin Invest* **82**, 594-600.
- Halperin JA, Taratuska A, Nicholson-Weller A (1993) Terminal complement complex C5b-9 stimulates mitogenesis in 3T3 cells. *J Clin Invest* **91**, 1974-1978.
- Hamilton KK, Sims PJ (1991) The terminal complement proteins C5b-9 augment binding of high density lipoprotein and its apolipoproteins A-I and A-II to human endothelial cells. *J Clin Invest* **88**, 1833-1840.
- Hamilton KK, Hattori R, Esmon CT, Sims PJ (1990)

Complement proteins C5b-9 induce vesiculation of the endothelial plasma membrane and expose catalytic surface for assembly of the prothrombinase enzyme complex. *J Biol Chem* **265**, 3809-3814.

Holme PA, Brosstad F, Solum NO (1993) The difference between platelet and plasma FXIII used to study the mechanism of platelet microvesicle formation. *Thromb Haemost* **70**, 681-686.

Holme PA, Solum NO, Brosstad F, Roger M, Abdelnoor M (1994) Demonstration of platelet-derived microvesicles in blood from patients with activated coagulation and fibrinolysis using a filtration technique and Western blotting. *Thromb Haemost* **72**, 666-671.

Holme PA, Solum NO, Brosstad F, Egberg N, Lindahl T (1995) Stimulated Glanzmann's thrombasthenia platelets produce microvesicles. Microvesiculation correlates better to exposure of procoagulant surface than to activation of GPIIb-IIIa. *Thromb Haemost* **74**, 1533-1540

Humphrey JH, Dourmashkin RR (1969) The lesions in cell membrane caused by complement. *Adv Immunol* **11**, 75-115.

Kerjaschki D, Schulze M, Binder S, Kain R, Ojha PP, Susani M, Horvat R, Baker PJ, Couser WG (1989) Transcellular transport and membrane insertion of the C5b-9 membrane attack complex of complement by glomerular epithelial cells in experimental membranous nephropathy. *J Immunol* **143**, 546-552.

Malinski JA, Nelsestuen GL (1989) Membrane permeability to macromolecules mediated by the membrane attack complex. *Biochemistry* **28**, 61-67.

Morgan BP, Dankert JR, Esser AF (1987) Recovery of human neutrophils from complement attack: Removal of the membrane attack complex by endocytosis and exocytosis. *J Immunol* **138**, 248-253.

Morgenstern E (1991) Aldehyde fixation causes membrane vesiculation during platelet exocytosis: A freeze-substitution study. *Scanning Microsc Suppl* **5**, 109-115.

Morgenstern E, Edelmann L (1989) Analysis of dynamic cell processes by rapid freezing and freeze substitution. In: *Electron Microscopy of Subcellular Dynamics*. Plattner H (ed.). CRC Press, Boca Raton, FL, pp 119-140.

Mueller-Eberhard HJ (1985) The killer molecule of complement. *J Invest Dermatol* **85** (Suppl. 1), 47S-52S.

Ornberg RL, Reese TS (1981) Beginning of exocytosis captured by rapid freezing of *Limulus* amoebocytes. *J Cell Biol* **90**, 40-54.

Peitsch MC, Amiguet P, Guy R, Brunner J, Maizel JV, Tschopp J (1990) Localization and molecular modeling of the membrane-inserted domain of the ninth component of human complement and perforin. *Mol Immunol* **27**, S89-602.

Podack ER (1992) Perforin: Structure, function, and regulation. *Curr Top Microbiol Immunol* **178**, 175-184.

Podack ER, Tschopp J (1984) Membrane attack by

complement. *Mol Immunol* **21**, 589-603.

Sims PJ, Wiedmer T (1986) Repolarization of the membrane potential of blood platelets after complement damage. Evidence for a Ca²⁺-dependent exocytotic elimination of C5b-9 pores. *Blood* **68**, 556-561.

Sims PJ, Faioni EM, Wiedmer T, Shattil SJ (1988) Complement proteins C5b-9 cause release of membrane vesicles from the platelet surface that are enriched in the membrane receptor for coagulation factor Va and express prothrombinase activity. *J Biol Chem* **263**, 18205-18212.

Sims PJ, Rollins SA, Wiedmer T (1989a) Regulatory control of complement on blood platelets. Modulation of platelet procoagulant responses by a membrane inhibitor of the C5b-9 complex. *J Biol Chem* **264**, 19228-19235.

Sims PJ, Wiedmer T, Esmon CT, Weiss HJ, Shattil SJ (1989b) Assembly of the platelet prothrombinase complex is linked to vesiculation of the platelet plasma membrane. *J Biol Chem* **264**, 17049-17057.

Sodetz JM (1988) Structure and function of C8 in the membrane attack sequence of complement. *Curr Top Microbiol Immunol* **140**, 19-31.

Solum NO, Rubach-Dahlberg E, Pedersen TM, Reisberg T, Hogasen K, Funderud S (1994) Complement-mediated permeabilization of platelets by monoclonal antibodies to CD9: Inhibition by leupeptin, and effects on the GP Ib-actin-binding protein system. *Thromb Res* **75**, 437-452.

Tranum-Jensen J, Bhakdi S (1983) Freeze-fracture analysis of the membrane lesion of human complement. *J Cell Biol* **97**, 618-626.

Tschopp J (1984) Ultrastructure of the membrane attack complex of complement. Heterogeneity of the complex caused by different degree of C9 polymerization. *J Biol Chem* **259**, 7857-7863.

Tschopp J, Masson D, Stanley KK (1986) Structural/functional similarity between proteins involved in complement- and cytotoxic T-lymphocyte-mediated cytolysis. *Nature* **322**, 831-834.

Wiedmer T, Sims PJ (1985) Effect of complement proteins C5b-9 on blood platelets: Evidence for reversible depolarization of the membrane potential. *J Biol Chem* **260**, 8014-8019.

Wiedmer T, Sims PJ (1991) Participation of protein kinases in complement C5b-9-induced shedding of platelet plasma membrane vesicles. *Blood* **78**, 2880-2886.

Wiedmer T, Shattil SJ, Cunningham M, Sims PJ (1990) Role of calcium and calpain in complement-induced vesiculation of the platelet plasma membrane and in the exposure of the platelet factor Va receptor. *Biochemistry* **29**, 623-632.

Young JD, Young TM (1990) Channel fluctuations induced by membrane attack complex C5B-9. *Mol Immunol* **27**, 1001-1007.

Discussion with Reviewers

W. van Oeveren: The release of granules from platelets results in decreased density of the cytosol and thus in increased light transmission in the aggregometer (Fig. 1). The authors explain the sequestration and release of granules by the permeabilization of the platelet membrane by the MAC complex. However, also an early effect after binding of MAC is the exposure of phosphatidylserine to the outer platelet membrane, which, together with released Factor V, potentiates the formation of thrombin on the platelet surface. Could it be possible that the processes following the initial shape change are induced (in part) by thrombin? Would a similar aggregation pattern be observed in the presence of a specific thrombin inhibitor?

Authors: We have carried out the experiment with FN 52 added to citrated PRP also anticoagulated with hirudin (20 U/ml) which is an inhibitor of thrombin. The aggregometer curves obtained did not differ from the curve shown in Figure 1. Simultaneous flow cytometric analyses showed the presence of microparticles. The shape change may be induced by ADP leaked out from the cytosol through the first pores in the membrane produced by the complement activation, or it may be a direct consequence of the introduction of some C5b-9 complexes, allowing Ca^{2+} ions to enter into the cell. In citrated plasma, as opposed to in ethylenediaminetetraacetic acid (EDTA) plasma, a significant amount of the calcium is present as free ions (Wiedmer and Sims, 1985), and a review by Deckmyn and DeReys (1995).

W. van Oeveren: The authors show a considerable time delay in this process from complement activation to platelet release (60 seconds). In circulating blood, this would mean a shedding of thrombogenic particles throughout the circulation with potential pathologic effects, specifically if platelets are not capable of aggregation, since active GPIIb/IIIa cannot be formed. Could the rapid formation of filopodia be responsible for localization of these phenomena *in vivo* to the site of inflammation?

Authors: The time delay from addition of FN 52 until the shape change occurs is believed to be related to the initial steps in complement activation. Thus, if the proteolytic inhibitor leupeptin, which inhibits these early steps, is added before FN 52 or immediately after, the whole process is prevented (Solum *et al.*, 1994). The shedding of microparticles starts during the shape change phase, and increases thereafter (Holme *et al.*, 1995). The microparticles possess a procoagulant surfaces and as suggested by the reviewer, they may therefore be thrombogenic. In line with this, we have demonstrated the presence of definite amounts of microparticles in blood from patients with disseminated intravascular coagulation (DIC) (Holme *et al.*, 1994). Their possible participation in in-inflammation is less clear, however.

W. van Oeveren: If a very limited number of MAC is formed on the platelet surface could it be eliminated by exocytosis without inducing this cascade of events resulting in platelet degranulation?

Authors: An enrichment of the microparticles with MAC has been shown after incorporation of this complex in the platelet membrane (Sims *et al.*, 1988). Binding of the antibody aE11 directed toward a neoepitope on C9, to microparticles was also observed as part of our recent flow cytometry analyses shown Figure 13. It may be speculated that this phenomenon represents a kind of defence against permeabilization at the early stage. As microparticle formation is always observed in association with a translocation of amino-phospholipids from the inner to the outer membrane leaflet, we have also speculated that this translocation may occur locally at the site of insertion of the complement complex leading to an instability resulting in the shedding of the particles. We have found particles with serrated contours associated with fragments (Figs. 7e, and 8b and 8c). In such a way, MAC might be removed from the platelet surface. Under the conditions of our experiments, this obviously did not prevent the platelet permeabilization resulting in platelet ghosts.

P.B. Bell: You discuss the observed decrease in cytosolic electron density as being caused by the “leaching of cytosolic components or by water influx into the cytosol.” Are these mutually exclusive, and what is the evidence that one or the other occurs?

Authors: As described in Solum *et al.* (1994), the FN 52 induced platelet reaction is accomplished by a moderate release of lactate dehydrogenase. This led to our assumption that water influx might be a reason for the decrease of cytosolic electron density. However, leaching of cytosolic components, particularly small ones, may occur simultaneously.

P.B. Bell: You mention the possibility that previous measurements of the dimension of MACs are smaller than the ones you observed because of aldehyde-induced shrinkage. What evidence supports this? Could shrinkage occur for other reasons as well, including dehydration?

Authors: It is well known that aldehydes, especially di-aldehydes, cause shrinkage of cells and their components by cross-linking (see for comparison Figs. 14a-14c). Of course, the drying process that is necessary during negative staining procedures may induce shrinkage. Regarding this study, shrinkage during dehydration using the cryosubstitution in acetone containing OsO_4 does not occur in a dimension worth mentioning. This was shown in a comparative study on muscle cells (Edelmann, 1989).

P.B. Bell: You mention possible interactions between the MACs and the cytoskeleton. What is the evidence for this and what is the functional significance of this interaction?

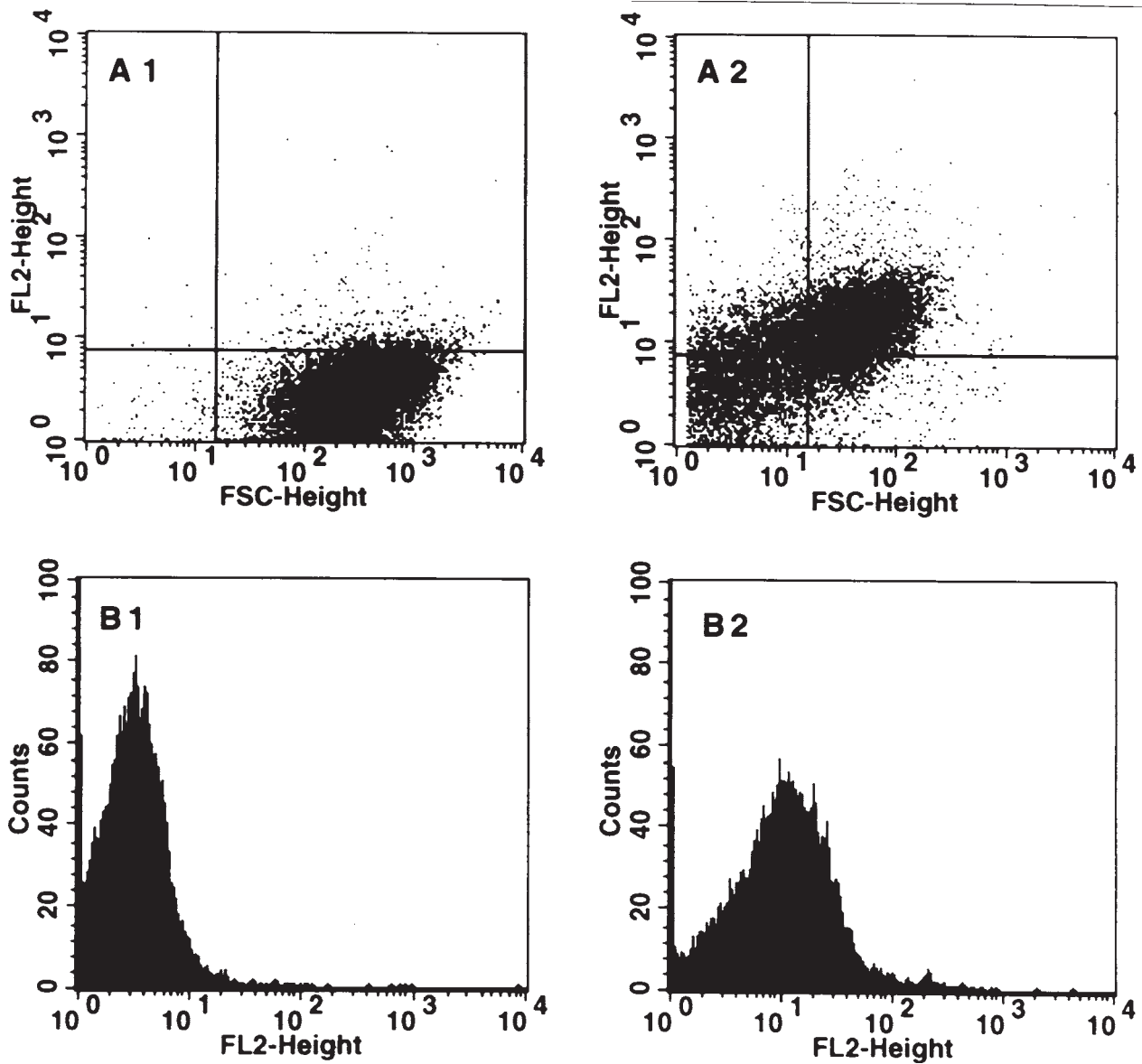


Figure 13. Flow cytometry of FN 52 treated platelets (A2 and B2) and untreated control cells (A1 and B1) using Mab aE11 directed to a neoepitope on C9 as primary antibody. Two color analysis was used: platelets were gated based on the fluorescence of a fluorescein isothiocyanate (FITC) labelled Mab against GPIIIa (FITC Y2/51). Detection of bound aE11 was done using a rPE labelled anti mouse IgG2a. The antibody M 5409 from Sigma (St. Louis, MO) was used as a negative control. **FSC** represents size, and **FL2** fluorescence intensity for each particle (i.e., platelet or microparticle). In panel **A2**, the fluorescence in the upper right quadrant demonstrates specific binding of aE11 to platelets, whereas binding to microparticles is shown to the left of the vertical line. Further, panel **B2** shows increased binding of aE11 to the stimulated platelets as compared to the unstimulated platelets in panel **B1**. The negative control M 5409 showed a fluorescence histogram identical to B1 after stimulation of the platelets with FN 52.

Authors: In rare cases, we have observed filamentous structures associated with dense deposits in our section series at the site of membrane irregularities. We have started immunolabeling experiments with antibodies either against

the MAC and precursor molecules or against actin and actin binding protein on sections of cryofixed and freeze-dried platelets to obtain detailed information regarding the interactions of MAC formation and the cytoskeleton. It is

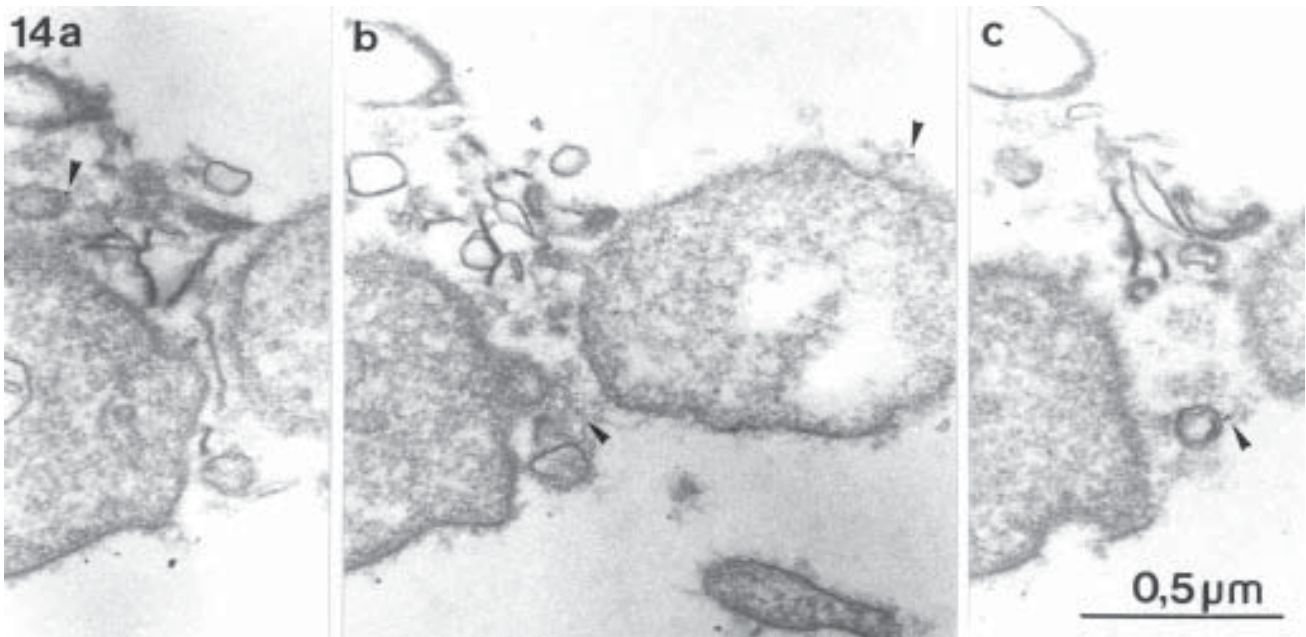


Figure 14 (a-c). Three consecutive sections from a platelet 60 seconds after FN 52 addition, prepared as described in the answer to Dr. Tranum-Jensen's last question, show labels indicating the antibody Mab aE11 directed to a neopeptide on C9 (arrowheads). Labels are seen on the surface of, or within, not clearly identifiable structures and myelin figures in the platelet surroundings (**Figs. 14a and 14c**) and on the surface of a shrunken platelet (**Fig. 14b**, left above). The medium is free of labels.

known that the generation of microparticles by C5b-9 is accompanied by proteolytic degradation of the cytoskeletal proteins actin binding protein, talin, and myosin heavy chain (Wiedmer *et al.*, 1990). As demonstrated in Figure 6 in Solum *et al.* (1994), sodium dodecyl sulfate-polyacrylamide gel electrophoresis (SDS-PAGE) and Western blotting showed an extensive degradation of the actin-binding protein at the end of the incubation under the conditions of the present experiments.

K. Ryan: This work shows a good use of rapid freezing where a specimen can be "immobilized" in a time period of less than a millisecond; the time during which freezing occurs at any one point being limited to about 250 microseconds, this being the ultimate limit for time resolution in cryofixation (modelled by Jones, 1984; Robards, 1984). The time steps of 24, 48, 60, 80 seconds and subsequent are probably well realized in your experimental results when you consider that aldehyde fixation can take 10 minutes to "fix" elongate cilia in tunicate structures, ending in pronounced artifactual "discocilia" (Bone *et al.*, 1982) and 15 minutes to "arrest" cytoplasmic movement in plant cells (Mersey and McCully, 1978; Robards, 1984). Do you think that, in the light of your results, most preceding work on the dynamic processes need reinvestigating using cryofixation?

Authors: Indeed, shortcomings of chemical fixation for investigation of cells have been reported in many studies. The most important handicaps are the long-lasting time of the arrest of cell functions, and the induction of artificial structures, excellently demonstrated in the study of Mersey and McCully (1978). A compilation of other examples, mainly regarding animal cells, was given in the text reference Morgenstern and Edelmann (1989). In the platelets fixed in suspension, the time of arrest after aldehyde fixation is, because of their small dimensions, surely shorter than in tissues or in plant cells surrounded by a cell wall. Nevertheless, also in small cells, aldehyde fixation cannot capture rapid dynamic events as membrane fusion or provide water movement (Morgenstern, 1991). In this context, a reinvestigation of such dynamic processes is a logical consequence.

K. Ryan: Could you comment further as to the angular appearance of the thin necks at the site of sequestration platelet fragments? Do you believe that your results suggest that the pseudopodia are extruded through the MAC?

Authors: The angular insertion of the neck lines in the membrane of the platelets, or of the fragments, is not compatible with the properties and the behavior of biological membranes. Therefore, we interpret these structures as being due to the MAC, and are able to show that their dimensions

may correspond with the MAC dimension. The neck lines (MAC?) connect the platelet plasmalemma with the membrane of the fragments at the time of sequestration, but this process is not comparable with a pseudopodia/filopodia formation. Filopodia formation, only observable during the first phase of platelet reaction, is a characteristic platelet response after activation.

R. Pipe: With your serial sections for Figure 3a (48 seconds after FN 52 addition), are there no pictures demonstrating long thin profiles of tube-like filopodia? If not all the circular profiles seen in Figure 3a are due to filopodia, what are the others due to if not sequestration of cytoplasmic fragments? Would scanning electron microscopy have been helpful for demonstrating the filopodia?

Authors: It was not possible to demonstrate a whole filopodium with this technique. We did not demonstrate pictures with long thin profiles of tube-like filopodia (which were present in other section series as elongated profiles) because we preferred to demonstrate in Figure 3 one of the rare examples of budding of a fragment. Thus, we demonstrate the filopodia by reconstruction. With scanning electron microscopy, it could be possible to show filopodia but surely not the formation of small fragments.

R. Pipe: Figure 6 (60 seconds after FN 52 addition) appears to show less pronounced changes in the alpha-granules than those in Figure 3 (48 seconds after FN 52 addition); can you explain why this might be?

Authors: Your comment is correct. Let us answer with the statement of J.G. White, a very experienced scientist in platelet morphology, who said “no two stimulated platelets are at exactly the same state of reaction at any moment in time.” Indeed, in some “leached” platelets some α -granules may be present. This phenomenon is also known from a few granule-containing platelets in a population that was stimulated with thrombin.

J. Tranum-Jensen: The study utilizes citrated PRP and a monoclonal Ab (FN 52) towards CD9 to induce formation of C5b-9 (MAC). The crucial question is of course if MAC is formed on the platelet membrane under these conditions. The present paper does not itself address this question but gives reference to Solum *et al.* (1994). The arguments given in this paper for formation of MAC on the platelets are that shape change and permeabilization (ATP release) of the platelets does not occur if plasma/serum is omitted, and that a serum depleted of C8 cannot fully replace the effects of full serum unless supplemented with purified C8. The first part of this argument is only valid if inactivated serum (56°C, 1 hour) does not elicit the effects.

Authors: This was the first we thought of when we started to suspect that the observed phenomenon might be due to

complement activation. We then performed experiments where isolated (washed) platelets were resuspended in either a citrated plasma, a plasma anti-coagulated using EDTA or a citrated plasma that had been “inactivated” by heating at 56°C for 30 minutes followed by removal of the precipitated fibrinogen by centrifugation. FN 52 was then added to each of these platelet suspensions in the aggregometer as in Figure 1 of our paper. The platelets in the citrated plasma showed the same aggregometer curve as in Figure 1. However, no reaction was observed with the platelets in the heat-inactivated plasma, or in the EDTA plasma. The interpretation of this is that in the last two cases, the membrane permeabilizing complement complex could not be produced. This is due to inactivation of necessary complement factors in the heat-inactivated plasma, and by the complexation of Ca^{2+} ions required for the complement activation when the EDTA plasma was used. Note again that the citrated plasma contains significantly more free Ca^{2+} ions than the EDTA plasma due to considerable differences in the complexation constants of these two calcium chelators.

J. Tranum-Jensen: The C8 supplementation-argument is somewhat hampered by the fact that the experiment is performed in the presence of calcium and absence of citrate.

Authors: It is not absolutely clear what the reviewer means. If he points to the fact that an experiment with washed platelets resuspended in a citrate-free serum with added Ca^{2+} ions, is not identical to experiments performed with platelets in citrated plasma, this obviously is correct as a general statement. However, there is no evidence to claim that FN 52 is not acting through the same mechanism in the two systems.

J. Tranum-Jensen: Measurement of extracellular C5b 9 is performed by an ELISA technique, but data are not shown, and the same applies to demonstration of C5b-9 on the platelet surface by flow cytometry.

Authors: The presence of the C5b-9 complex on the platelet surface after FN 52 addition was demonstrated by flow cytometry using the same monoclonal antibody to a neo-epitope on C9 (Mab aE11) as used for the ELISA-technique. The ELISA results are shown here in Table 1 and Figure 15, and the flow cytometry data in Figure 13.

Corresponding data were shown in a poster presentation at the XIIIth Congress of the International Society of Haemostasis and Thrombosis, Amsterdam, The Netherlands, 1991, but were not published elsewhere. The flow cytometry has been re-evaluated in connection with the revision of the present paper using the more sophisticated approach of dual labelling which has the advantage that also microparticles can be studied.

In addition, Table 1 also shows the values for the determination of the C3 conversion, requested in the next paragraph. The monoclonal antibody aE11 directed to a

Table 1. Measurements of the sC5b-9 complex and C3 activation products (C3bc) present extracellularly after platelet alteration induced by FN 52, and demonstration of the effect of leupeptin on these products.

Curves*	FN52 (IgM)	Leupeptin (1.6 mM)	sC5b-9 (AU/ml)	C3b-9 C3bc (AU/ml)
1	Present	Absent	3.3	10.3
2	Present	Present	2.2	5.2
3	Absent	Absent	1.5	3.9

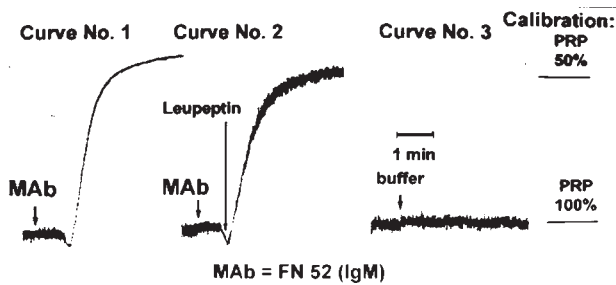


***Figure 15.** The three aggregometer curves corresponding to Table 1 are also shown. Note that in curve 2, leupeptin was added during the shape change phase.

neoepitope on C9 was used both in Table 1 and Figure 13. This antibody has been described in detail in a previous paper (Mollnes *et al.*, 1985).

J. Tranum-Jensen: Complement activation in general should be monitored, e.g., by measuring C3 conversion.

Authors: We did these measurements also, but without publishing them. Actually, in parallel with the measurements of the ELISA determinations of soluble C5b-9 (sC5b-9) discussed above, we also did ELISA measurements of the C3 activation products stated as C3bc (C3b + inactivated C3b + C3c) in exactly the same samples. The results parallel those of the C5b-9 values, and go well along with the idea of complement activation. You will find these values added in Table 1. These measurements were done on at least two occasions, each time with 9 wells for each sample.

J. Tranum-Jensen: Various other indirect lines of evidence point to MAC formation on the platelet surface, but I am missing compelling evidence that MAC is formed on/in platelet membrane, e.g., by immunolabelling microscopy using an antibody towards a C9 neoantigen, or even better by clear demonstration of characteristic complement lesions by negative staining, ideally supplemented with immunogold labelling.

Authors: During experiments in Oslo, Norway, we also have used the preembedding-labelling technique to find the MAC on washed platelets 60 seconds after addition of FN 52. For this experiment, the platelets were fixed with a buffered solution containing 2% paraformaldehyde and 0.2% glutaraldehyde, incubated for 10 minutes at 37°C with the primary antibody Mab aE11 directed to a neoepitope on C9 (the same as used in Table 1 and Fig. 13). After washing, a 6 nm, gold-labeled anti-mouse IgG was added, and the incubation was continued at room temperature for 1 hour. Then, pellets were postfixed with OsO₄ according to Caulfield (1957), dehydrated and embedded in Araldite. The results are demonstrated in Figures 14a-14c. Thus, also by transmission electron microscopy, we have evidence that the MAC is present on the platelet membrane after induction. On the other hand, the micrographs demonstrate the inability of aldehyde fixation to preserve the platelet reactions during MAC-formation as shown in the paper. We hesitated to present such micrographs because of the poor standard of preparation. Holes in cell membranes caused by MAC-formation were elegantly demonstrated by the reviewer (Fig. 7 in text reference Bhakdi and Tranum-Jensen, 1986) and by many others. Because we know that the MAC was present in the experiments, and permeabilization took place, we did not work with preparation of negatively stained platelet membranes, a technique in which we are not experienced.

Additional References

- Bone Q, Ryan KP, Pulsford AL (1982) The nature of complex discocilia in the endostyle of *Ciona* (Tunicata Ascidiacea). *Mikroskopie (Wien)* **39**, 149-153.
- Caulfield JB (1957) Effects of varying the vehicle for osmium tetroxide in tissue fixation. *J Biophys Biochem Cytol* **3**, 287.
- Deckmyn H, DeReys S (1995) Functional effects of human anti-platelet antibodies. *Semin Thromb Hemost* **21**, 46-59.
- Jones GJ (1984) On estimating freezing times during tissue rapid freezing. *J Microsc* **136**, 349-360.
- Mersey B, McCully ME (1978) Monitoring the course of time fixation in plant cells. *J Microsc* **114**, 49-76.
- Mollnes TE, Lea T, Harboe M, Tschopp J (1985) Monoclonal antibodies recognizing a neoantigen of poly(C9)

Membrane attack complex on platelets

detect the human terminal complement complex in tissue and plasma. *Scand J Immunol* **22**, 183-195.

Robards A W (1984). Fact or artifact: A cool look at biological electron microscopy. *Proc Royal Microsc Soc* **19**, 195-208.